ISSN 0915-633X

NATIONAL INSTITUTE FOR FUSION SCIENCE

Dynamic Behavior of Potential in the Plasma Core of the CHS Heliotron/Torsatron

A. Fujisawa, H. Iguchi, H. Sanuki, K. Itoh, S. Lee, Y. Hamada, S. Kubo, H. Idei, R. Akiyama, K. Tanaka, T. Minami, K. Ida, S. Nishimura, S. Morita, M. Kojima, S. Hidekuma, S.-I. Itoh, C. Takahashi, N. Inoue, H. Suzuki, S. Okamura and K. Matsuoka

(Received - Mar. 18, 1997)

NIFS-488 Apr. 1997

RESEARCH REPORT
NIFS Series

NAGOYA, JAPAN

Dynamic Behavior of Potential in the Plasma Core of the CHS Heliotron/Torsatron

A. Fujisawa, H. Iguchi, H. Sanuki, K. Itoh, S. Lee, Y. Hamada, S. Kubo, H. Idei, R. Akiyama, K. Tanaka, T. Minami, K. Ida, S. Nishimura, S. Morita, M. Kojima, S. Hidekuma, S.-I. Itoh*, C. Takahashi, N. Inoue, H. Suzuki, S. Okamura, K. Matsuoka

National Institute for Fusion Science, Furo-cho, Chikusa-ku, Nagoya 464-01, Japan

**RIAM, Kyushu University, Kasuga 816, Japan*

(March 18, 1997)

Abstract

During a combined heating phase of ECH and NBI, an abrupt drop and rise in potential by about a half of central electron temperature ($\sim$ 400 V) was observed in the core of the CHS heliotron/torsatron plasma. Drastic changes of radial electric field between positive and negative states occur in 50 μs at shortest, which is much shorter than the energy confinement time scale of about a few milliseconds. Nonlinear relation between the radial electric field and radial current is obtained. This is the first experimental observation of a spontaneous transition based on an electric field bifurcation in microseconds order in toroidal helical plasmas.

Keywords: Spontaneous transition, Electric field, Bifurcation, Nonlinear E-J curve, Toroidal Helical Plasma, Heavy Ion Beam Probe

Structural formation of radial electric field in toroidal plasmas, such as tokamaks and stellarators, is a key physics issue associated with improved confinement modes, such as H-mode [1,2]. It has been discussed that the origin of the L-H mode transition should be ascribed to a change in the structure of radial electric field near the plasma edge [3,4]. A nonlinear dependence of plasma confinement on radial electric field should cause a bifurcation into two quite different states of better and worse confinement [5].

For toroidal helical plasmas, an absolute value of radial electric field is intrinsically influential to the confinement, since the helical ripple induced transport and loss cone loss are sensitive to structure of the radial electric field. The neoclassical analysis has already shown that toroidal helical plasmas bifurcate into two states and possess a possibility of existence of a solitary wave in the radial electric field [6,7]. This nonlinearity inherent in toroidal helical plasmas gives rise to dynamic and drastic behavior in the radial electric field. The formation mechanism of radial electric field, therefore, is essentially governed by nonlinearity which is one of the main subjects of modern physics.

Heavy ion beam probe (HIBP) is a diagnostic to measure directly the internal plasma potential [8–10] with a high temporal and spatial resolution. A 200keV HIBP [11,12] is installed on the Compact Helical System (CHS), which is a heliotron/torsatron device of medium size; its major and averaged minor radii are 1.0m and 0.2m, respectively, and its periodicity is toroidally 8, and poloidally 2 [13]. In the first results with the HIBP, the potential profiles of steady states exhibited widely varying characteristics for electron cyclotron heating (ECH) and neutral beam injection (NBI) plasmas [14].

In the previous CHS experiments, a change of electric field at $\rho(= r/a) \simeq 0.8$, from negative to positive, was deduced when an extra electron flux was induced with a use of ECH local heating [15,16]. The electric field was evaluated from Charge Exchange Recombination Spectroscopic (CXS) measurements with a temporal resolution of about 17ms. However, the temporal resolution was too long to identify the transition nature of the electric field. The temporal resolution of the HIBP allows us to catch up with a rapid change of the potential in microseconds order, and gives detail information about the transition phase of electric

field. In this letter, we will describe dynamics of the transition of the radial electric field in the plasma core of the CHS plasma during a combined heating phase of ECH+NBI, and we will present nonlinear dependence of radial current on radial electric field to cause this bifurcation phenomenon.

The experiments presented here were performed at magnetic field configuration whose magnitude and axis position were 0.9T and 92.1cm, respectively. The working gas was deutrium and the injected neutral beam was hydrogen. A 300kW gyrotron of 53.2GHz was used to produce target plasmas with its resonance position on the magnetic axis. After the pure ECH phase, the NBI with port-through power of 800kW was superposed on the plasma. Electron temperature profiles were measured with a YAG Thomson scattering system with a repetition rate of 10ms. Ion temperature profile was obtained with a CXS system. Line averaged electron density was monitored in two chords with HCN interferometers. The observable range of the HIBP covers almost all magnetic flux surfaces [11,12] of this magnetic configuration. The HIBP signal is acquired with a sampling rate of 1μs. The current amplifier has a frequency band up to 450kHz. The amplifier noise gives the false potential fluctuation with the amplitude of $\sim$ 20V in the present experiments. The HIBP has a capability to observe three spatially adjacent points simultaneously using three beam current detectors.

In the ECH heating phase, the central electron temperature is about 800$\pm$200eV, and the line averaged electron density $\bar{n}_e$ is $3 \times 10^{12}\mathrm{cm}^{-3}$. In this combined heating phase, the electron density gradually increases from $3 \times 10^{12}\mathrm{cm}^{-3}$ at $t = 50$ms to $6 \times 10^{12}\mathrm{cm}^{-3}$ at $t = 70$ms. No significant difference in electron temperature was seen in the repetition rate of YAG Thomson scattering, while the central ion temperature increases approximately from 100eV to 300eV.

Figure 1 shows time evolutions of potential at several fixed spatial points (a), and potential profiles (b) taken in ECH, ECH+NBI and NBI phases by radially scanning. A radial scan took about 9ms in this case. In the pure ECH phase (A), the potential profile has a sharp peak in the core of $\rho < 0.3$ (open circles in Fig. 1b). Negative ρ in Fig. 1b means that

the observation point is located below the magnetic axis. Just after NBI is turned on, the central potential increases with the time scale of 1ms by ($\Delta\phi(0)$ =)200V, while no significant change is seen in other spatial points. Then the central potential gradually decreases, accompanied with a sudden drop (t = 54.5ms) and rise (t = 56.0ms) in the core potential. On the other hand, the potential near the plasma edge monotonically decreases, and the electric field of $\rho > 0.8$ turns negative in about 5 ms. In the later period of the combined heating phase (B), the potential profile develops into a shape like 'Mexican hat'(closed circles in Fig. 1b); the radial scan is performed from t = 59ms to t = 68ms. The potential profile similar to this shape has been observed in 100kW ECH heated plasmas with $\bar{n}_e$ of $8 \times 10^{12}\mathrm{cm}^{-3}$ [14]. After the ECH is turned off, the plasma starts to relax into the steady state potential profiles (squares in Fig. 1c) in NBI plasmas in 1$\sim$2 ms.

Spatial and temporal structure of the drastic change in the core potential, being denoted 'transition' in Fig. 1a, should be examined in more detail. Figure 2a demonstrates potential changes at several spatial points, when the observation points are fixed during a shot. The dashed line represents potential profiles taken in radial scan during an initial phase of ECH+NBI heating as a reference. The data was taken from the sequential shots under the identical operational condition. The open squares and closed circle are potential values before and after the transition, respectively(see the arrows in Fig. 2b). Within the experimental results we have obtained so far, this dynamic behavior is limited in the core of $\rho < 0.4$. This figure suggests that the profile with the sharp peak turns into a flat or hollow profile. It is difficult to obtain the fine structural change of profile during the transition, which is happening in a few dozen microseconds. The differences between potential signals from three detectors, which simultaneously observe spatially adjacent points, show to change their signs. These observations imply that the electric field changes from positive to negative. An increase in the magnetic field fluctuation was detected in a certain poloidal position just around the time of the transition, although the causality needs further investigation.

Figure 2b shows an expanded view of the rapid rise and drop in the core potential($\rho = 0$), together with detected beam current (signal) intensity. The time scale of the potential change

can be examined in more detail by fitting a function of $\phi(t,\ \rho = 0) = 0.5\Delta\phi[\tanh\ ((t - t_0)\tau^{-1}) + 1] + \phi_0$ to the wave form in the transient phase. The fitting parameters for the abrupt drop and rise are $\Delta\phi(\rho = 0) = -179$ V, $\tau = 60\mu$s, $t_0 = 54.6$ms, and $\Delta\phi(\rho = 0) = 395$ V, $\tau = 220\mu$s, $t_0 = 56.0$ms, respectively. The solid lines indicate the fitting curves.

The signal intensity detected with the HIBP exhibits the increase and decrease correlated with the potential drop and rise in a similar time scale. This suggests that the electron density profile is changing in a very local region, however, no significant change in line averaged density is observed with the interferometer during this rapid change. The signal intensity $I_{\rm D}$ is expressed as $I_{\rm D}(r) \propto Q_{12}(r)\exp[-\int_{\rm edge}^{r} Q_1 {\rm d}l_1 - \int_{r}^{\rm edge} Q_2 {\rm d}l_2]$, where $Q_{12}(r)(\propto n_{\rm e}(r))$ represents local ionization rate from singly charged state to doubly one. The exponential term represents the beam attenuation along the beam trajectory, with Q_1 and Q_2 being the total ionization crossections from the singly charged state and that from the doubly one, respectively. The relation of $\Delta Q_{12}/Q_{12} \simeq \Delta n_{\rm e}/n_{\rm e}$ indicates the local electron density increases by 15% at $t_0 = 54.6$ms, and decreases by 30% at $t_0 = 56.0$ms, being accompanied with the structural change of the radial electric field. The order of density change is estimated to be $\sim 10^{12}{\rm cm}^{-3}$.

The radial electric field change is induced by radial current, which produces the $j \times B$ force to make the plasma rotate. As a result, the time scale of the transition is connected to the magnitude of the radial current in the following way [5],

$$j_{\rm r}(E_{\rm r}) = -\varepsilon_\perp \varepsilon_0 \frac{\partial E_{\rm r}}{\partial t} \ , \qquad (1)$$

where $\varepsilon_\perp$ represents the perpendicular dielectric constant of the plasma, with ε_0 being the vacuum dielectric constant. The perpendicular dielectric constant is given by $\varepsilon_\perp = M_{\rm tor}(1 + c^2/v_{\rm A}^2)$, where c and $v_{\rm A}$ are light and Alfven velocities, respectively. The toroidal enhancement factor is simply estimated as $M_{\rm tor} \simeq 1 + 2q^2$, where q is the safety factor; q-profile of the CHS is approximately expressed as $q = 3.3 - 3.8\rho^2 + 1.5\rho^4 + \cdots$ in a polynomial series.

The radial current change can be estimated by using Eq. (1). We assume that the Alfven

velocity is 8×10^6m/s, which corresponds to the electron density $n_e = 3 \times 10^{12}\text{cm}^{-3}$. The perpendicular dielectric constant is $\varepsilon_\perp \simeq 2.7 \times 10^4$ when $q \simeq 3$. We will use an average field instead of the local radial electric field in the following analysis, since the exact change of the local electric field is difficult to be obtained. The average radial electric field is given by $\bar{E}_r = -[\phi(0.3a) - \phi(0)]/0.3a$,

Using a wavelet analysis on the estimated average electric field, we evaluate the radial current in Fig. 3a. The maximum currents are $4.5 \pm 3.0\text{A/m}^2$ and $-3.6 \pm 2.4\text{A/m}^2$ for the transitions at $t = 54.6$ms and $t = 56.0$ms, respectively. The error bars in the electric field and radial currents come from uncertainty of potential change at $\rho = 0.3$. Figure 3b plots the radial current as a function of the radial electric field (E-J curve) using the wavelet analysis. The dashed line represents the E-J curve obtained from the fitting function in Fig. 2b. This difference represents the uncertainty owing to the fitting fuctions. These two curves unambiguously demonstrates nonlinear relationship between the radial current and radial electric field, that realizes the transition of the radial electric field. When the plasma is in the state A (or C) in Fig. 3c, a slightly positive (or negative) change in the electric field drives the plasma to move from the original state to another B (or D). This is because the induced current is in the direction to increase the change of the electric field.

It is of some interest to compare the observed current with the estimate based on the neoclassical theory [17–19]. The neoclassical contribution could be dominant within various mechanisms to determine the radial electric field for the present experiments [5]. Figure 3c indicates two examples of the radial current as a function of radial electric field when the bifurcation condition is satisfied for plausible parameters of the CHS plasma. The expression of fluxes given by Hastings et al. [18] is used in this calculation. The profiles of temperature and electron density in calculation are assumed to be all parabolic, with the central values being 350eV and $5 \times 10^{12}\text{cm}^{-3}$. The central electron temperature is assumed to be 630eV and 800eV for cases of (I) and (II).

The calculated radial current $\sim 5\text{A/m}^2$ is within the range of the experimental value. And the topology of the E-J curve is identical with the experiment. The width of expected

electric field change from state (C′) to (D′) is larger than that from (A′) to (B′). This property of the width is qualitatively agreed with the experiment. The essential conclusion obtained here remains the same if we choose another density profile. With an assumption of flat density profile, the neoclassical estimate of radial current is different from the parabolic case approximately by 50%.

In the CCT and the TEXTOR tokamaks [20,21], L-H mode transition was achieved by producing electric field using biasing electrodes inserted into the plasma edge. Relationship between applied voltage and induced radial current is obtained, and a gap in the radial current is seen at the electric field where the 'forced' transition occurs [21]. On the other hand, the E-J curve we presented here is obtained for a 'spontaneous' transition where no external disturbance exists.

Finally, another interesting discovery is the potential profile having sharp peak in the ECH heating phase. The radial electric fields inside and outside of this boundary are estimated about 50V/cm and 20V/cm, respectively, and the corresponding $E \times B$ drift velocities are 6km/s and 2km/s. The existence of steep gradients in the electric field and velocity at $\rho = 0.3 \sim 0.4$ suggests a momentum transport barrier. The detail about this prominent profile will be discussed in another article.

In conclusion, we have observed a spontaneous transition in a toroidal helical plasma. During a combined heating phase of ECH+NBI, the steep gradient of potential is destroyed and recovered in a few dozen or hundred microseconds by achieving a bifurcation condition. It has been experimentally confirmed for the first time that the E-J curve in the toroidal helical plasma has nonlinear characteristics to allow of bifurcation in the radial electric field. The radial current governing the time scale of the transition is estimated experimentally to be about 5 A/m^2, which is found in the order of the neoclassical calculation. The HIBP signals imply that this radial electric field change is accompanied by a local electron density change. We have successfully observed nature of the spontaneous transition in the radial electric field, and this observation gives a new insight to structural formation of radial electric field in toroidal plasmas.

REFERENCES

[1] F. Wagner et al., Phys. Rev. Lett. **49** 1408(1982).

[2] ASDEX Team, Nucl. Fusion **29** 1959(1989).

[3] S.-I. Itoh, K. Itoh, Phys. Rev. Lett. **60** 2276(1988).

[4] K. C. Shaing, E. Crume Jr., Phys. Rev. Lett. **63** 2369(1989).

[5] For review, e.g., K. Itoh, S.-I. Itoh, Phys. Contr. Fusion **38**, 1(1996).

[6] D. E. Hastings, R. D. Hazeltine and P. J. Morrison, Phys. Fluids **29**, 69(1986).

[7] E. Yahagi, K. Itoh, M. Wakatani, Plasma. Phys. Contr. Fusion. **30**, 995(1988).

[8] F. C. Jobes, R. L. Hickok, Nucl. Fusion **10** 195(1970).

[9] G. A. Hallock, J. Mathew, W. C. Jennings *et al.*, Phys. Rev. Lett. **56** 1248(1986).

[10] X. Z. Yang, B. Z. Zhang, A. J. Wootton, *et al.*, Phys. Fluids B **3** 3448(1991).

[11] A. Fujisawa, H. Iguchi, M. Sasao, Y. Hamada, J. Fujita, Rev. Sci. Instrum. **63** 3694(1992).

[12] A. Fujisawa, H. Iguchi, S. Lee *et al.*, Rev. Sci. Instrum. **67** 3099(1996).

[13] K. Matsuoka, S. Kubo, M. Hosokawa, et al., *in Plasma Physics and Controlled Nuclear Fusion Research 1988* (Proc. 12th Int. Conf. Nice, 1988), International Atomic Energy Agency, Vienna,1989, Vol. 2, 411.

[14] A. Fujisawa, H. Iguchi, *et al.*, Phys. of Plasmas(1997) in press.

[15] H. Idei, K. Ida, H. Sanuki *et al.*, Phys. Rev. Lett. **71** 2220(1993).

[16] H. Sanuki, K. Itoh, J. Todoroki et al., Physica Scripta **52** 461(1995).

[17] H. Sanuki, K. Itoh, S.-I. Itoh, J. Phys. Soc. Jpn. **62**, 123(1993).

[18] D. E. Hastings, W. A. Houlberg, K. C. Shaing, Nucl. Fusion **25** 445(1985).

[19] L. M. Kovrizhnykh, Nucl. Fusion **24**. 435(1984).

[20] R. J. Taylor, M. L. Brown, B. D. Fried. et al., Phys. Rev. Lett. **63** 2365(1989).

[21] R. R. Weynants, G. Van Oost, G. Bertschinger, et al., Nucl. Fusion **32** 837(1992).

FIGURES

FIG. 1. (a) Time evolution of potential for several spatial points. (b) Potential profiles measured in radial scanning. The open circles, closed circles and squares represent potential profiles during ECH phase (A), combined heating phase of ECH+NBI (B), and NBI phase (C), respectively.

FIG. 2. (a) Potential profile around $t = 54$ms obtained in scanning mode. The potential changes at several spatial points from $t = 54.5$ms to $t = 55$ms are also shown. (b) Time evolution of $\phi(0)$, and the fitting to the sudden drop and rise, together with time evolution of signal intensity.

FIG. 3. (a) Experimental radial current to induce electric field change. The solid and dashed lines show the radial current and electric field, respectively. (b) Experimental radial current $j_{\rm r}$ as a function of radial electric field $E_{\rm r}$. The open circles are plotted in every 64μs. (c) Diagram of calculated radial electric field and radial current using a neoclassical formula. This diagram show critical conditions to cause transition based on bifurcation.

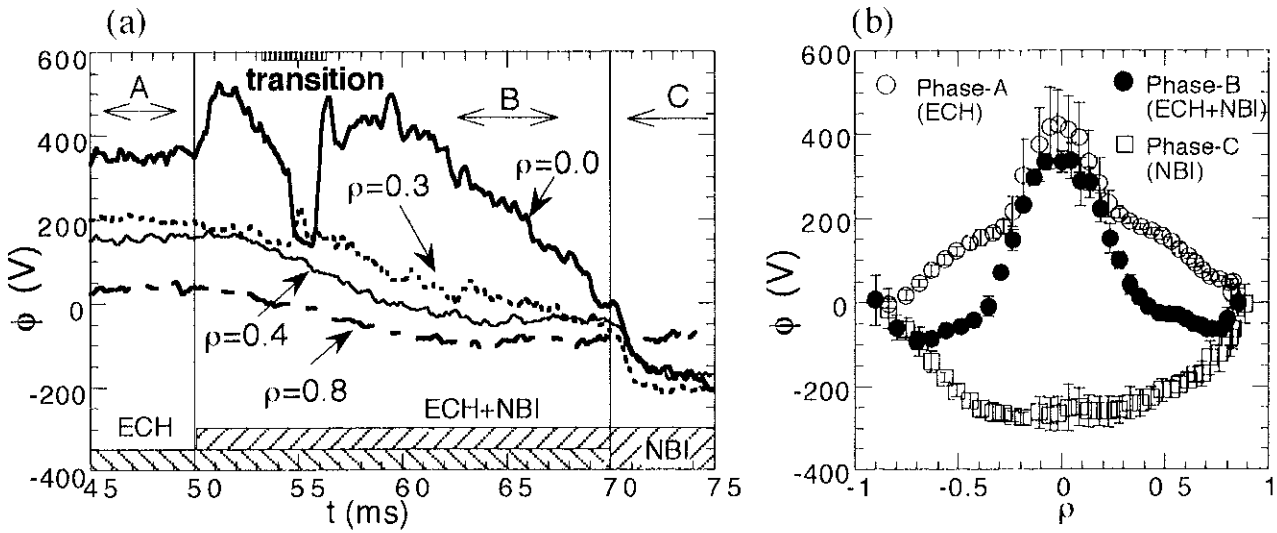

Figure 1 A Fujisawa et al

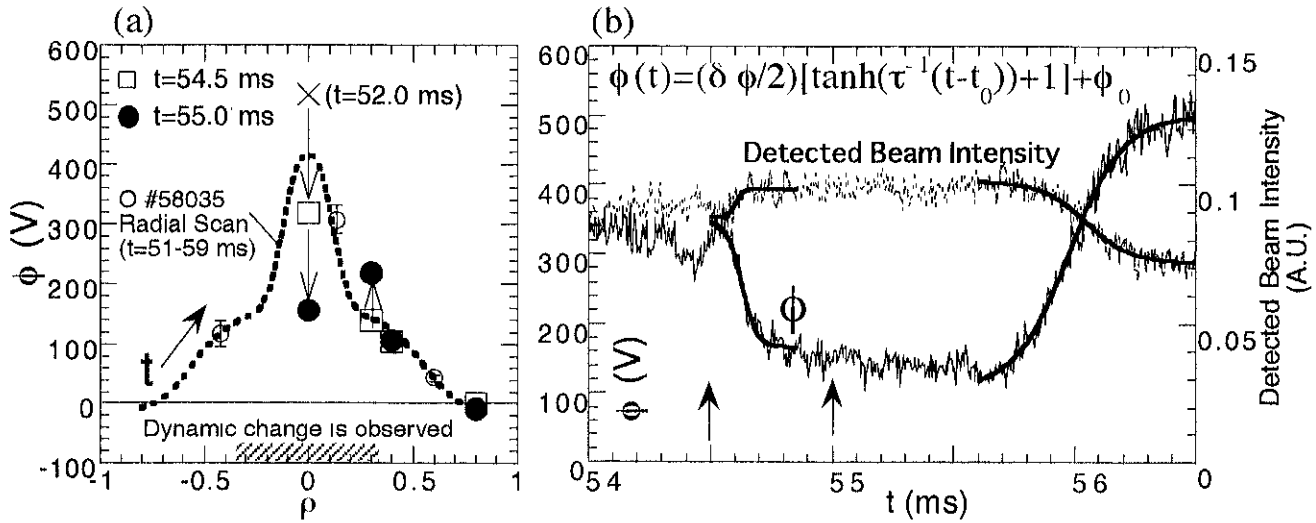

Figure 2 A. Fujisawa et al.

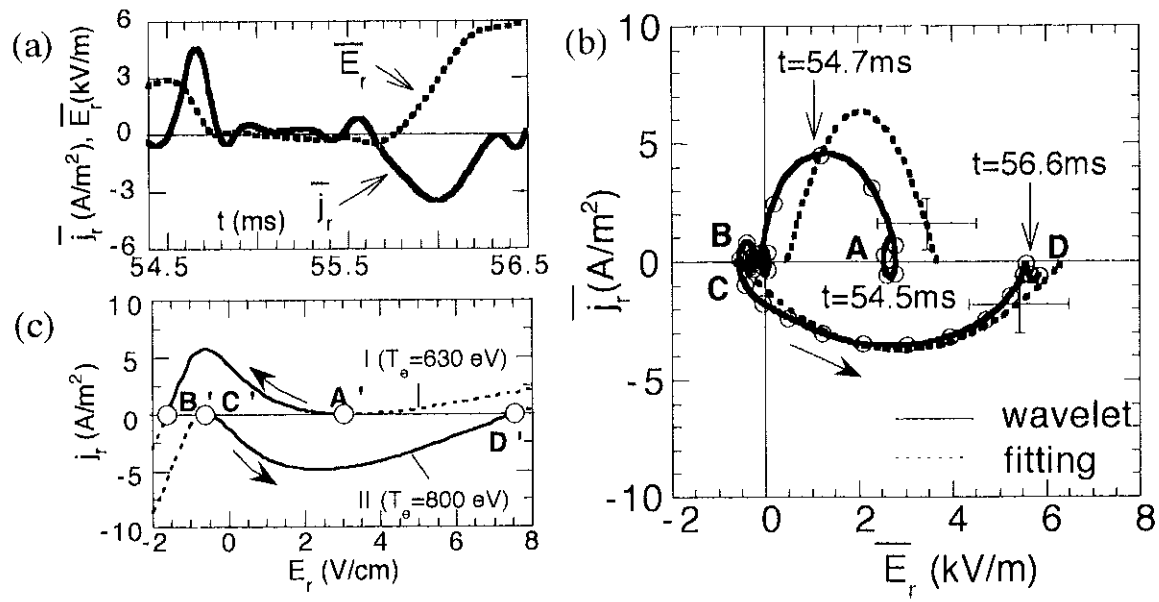

Figure 3 A Fujisawa et al.

Recent Issues of NIFS Series

NIFS-445 O. Motojima, N. Yanagi, S. Imagawa, K. Takahata, S. Yamada, A. Iwamoto, H. Chikaraishi, S. Kitagawa, R. Maekawa, S. Masuzaki, T. Mito, T. Morisaki, A. Nishimura, S. Sakakibara, S. Satoh, T. Satow, H. Tamura, S. Tanahashi, K. Watanabe, S. Yamaguchi, J. Yamamoto, M.Fujiwara and A. Iiyoshi,
Superconducting Magnet Design and Construction of LHD; Sep. 1996 (IAEA-CN-64/G2-4)

NIFS-446 S. Murakami, N. Nakajima, S. Okamura, M. Okamoto and U. Gasparino,
Orbit Effects of Energetic Particles on the Reachable β–Value and the Radial Electric Field in NBI and ECR Heated Heliotron Plasmas; Sep. 1996 (IAEA-CN-64/CP -6) Sep. 1996

NIFS-447 K. Yamazaki, A. Sagara, O. Motojima, M. Fujiwara, T. Amano, H. Chikaraishi, S. Imagawa, T. Muroga, N. Noda, N. Ohyabu, T. Satow, J.F. Wang, K.Y. Watanabe, J. Yamamoto , H. Yamanishi, A. Kohyama, H. Matsui, O. Mitarai, T. Noda, A.A. Shishkin, S. Tanaka and T. Terai
Design Assessment of Heliotron Reactor; Sep. 1996 (IAEA-CN-64/G1-5)

NIFS-448 M. Ozaki, T. Sato and the Complexity Simulation Group,
Interactions of Convecting Magnetic Loops and Arcades; Sep. 1996

NIFS-449 T. Aoki,
Interpolated Differential Operator (IDO) Scheme for Solving Partial Differential Equations; Sep. 1996

NIFS-450 D. Biskamp and T. Sato,
Partial Reconnection in the Sawtooth Collapse; Sep. 1996

NIFS-451 J. Li, X. Gong, L. Luo, F.X. Yin, N. Noda, B. Wan, W. Xu, X. Gao, F. Yin, J.G. Jiang, Z. Wu., J.Y. Zhao, M. Wu, S. Liu and Y. Han,
Effects of High Z Probe on Plasma Behavior in HT-6M Tokamak; Sep. 1996

NIFS-452 N. Nakajima, K. Ichiguchi, M. Okamoto and R.L. Dewar,
Ballooning Modes in Heliotrons/Torsatrons; Sep. 1996 (IAEA-CN-64/D3-6)

NIFS-453 A. Iiyoshi,
Overview of Helical Systems; Sep. 1996 (IAEA-CN-64/O1-7)

NIFS-454 S. Saito, Y. Nomura, K. Hirose and Y.H. Ichikawa,
Separatrix Reconnection and Periodic Orbit Annihilation in the Harper Map; Oct. 1996

NIFS-455 K. Ichiguchi, N. Nakajima and M. Okamoto,
Topics on MHD Equilibrium and Stability in Heliotron / Torsatron; Oct. 1996

NIFS-456 G. Kawahara, S. Kida, M. Tanaka and S. Yanase,

Wrap, Tilt and Stretch of Vorticity Lines around a Strong Straight Vortex Tube in a Simple Shear Flow; Oct. 1996

NIFS-457 K. Itoh, S.- I. Itoh, A. Fukuyama and M. Yagi,
Turbulent Transport and Structural Transition in Confined Plasmas; Oct. 1996

NIFS-458 A. Kageyama and T. Sato,
Generation Mechanism of a Dipole Field by a Magnetohydrodynamic Dynamo; Oct. 1996

NIFS-459 K. Araki, J. Mizushima and S. Yanase,
The Non-axisymmetric Instability of the Wide-Gap Spherical Couette Flow; Oct. 1996

NIFS-460 Y. Hamada, A. Fujisawa, H. Iguchi, A. Nishizawa and Y. Kawasumi,
A Tandem Parallel Plate Analyzer; Nov. 1996

NIFS-461 Y. Hamada, A. Nishizawa, Y. Kawasumi, A. Fujisawa, K. Narihara, K. Ida, A. Ejiri, S. Ohdachi, K. Kawahata, K. Toi, K. Sato, T. Seki, H. Iguchi, K. Adachi, S. Hidekuma, S.Hirokura, K. Iwasaki, T. Ido, M. Kojima, J. Koong, R. Kumazawa, H. Kuramoto. T. Minami, I. Nomura, H. Sakakita, M. Sasao, K.N. Sato, T. Tsuzuki, J. Xu, I. Yamada and T. Watari,
Density Fluctuation in JIPP T-IIU Tokamak Plasmas Measured by a Heavy Ion Beam Probe; Nov. 1996

NIFS-462 N. Katsuragawa, H. Hojo and A. Mase,
Simulation Study on Cross Polarization Scattering of Ultrashort-Pulse Electromagnetic Waves; Nov. 1996

NIFS-463 V. Voitsenya, V. Konovalov, O. Motojima, K. Narihara, M. Becker and B. Schunke,
Evaluations of Different Metals for Manufacturing Mirrors of Thomson Scattering System for the LHD Divertor Plasma; Nov. 1996

NIFS-464 M. Pereyaslavets, M. Sato, T. Shimozuma, Y. Takita, H. Idei, S. Kubo, K. Ohkubo and K. Hayashi,
Development and Simulation of RF Components for High Power Millimeter Wave Gyrotrons; Nov. 1996

NIFS-465 V.S. Voitsenya, S. Masuzaki, O. Motojima, N. Noda and N. Ohyabu,
On the Use of CX Atom Analyzer for Study Characteristics of Ion Component in a LHD Divertor Plasma; Dec. 1996

NIFS-466 H. Miura and S. Kida,
Identification of Tubular Vortices in Complex Flows; Dec. 1996

NIFS-467 Y. Takeiri, Y. Oka, M. Osakabe, K. Tsumori, O. Kaneko, T. Takanashi, E. Asano, T. Kawamoto, R. Akiyama and T. Kuroda,
Suppression of Accelerated Electrons in a High-current Large Negative Ion Source; Dec. 1996

NIFS-468 A. Sagara, Y. Hasegawa, K. Tsuzuki, N. Inoue, H. Suzuki, T. Morisaki, N. Noda, O. Motojima, S. Okamura, K. Matsuoka, R. Akiyama, K. Ida, H. Idei, K. Iwasaki, S. Kubo, T Minami, S. Morita, K. Narihara, T. Ozaki, K. Sato, C. Takahashi, K. Tanaka, K. Toi and I. Yamada,
Real Time Boronization Experiments in CHS and Scaling for LHD, Dec. 1996

NIFS-469 V.L. Vdovin, T.Watari and A. Fukuyama,
3D Maxwell-Vlasov Boundary Value Problem Solution in Stellarator Geometry in Ion Cyclotron Frequency Range (final report); Dec. 1996

NIFS-470 N. Nakajima, M. Yokoyama, M. Okamoto and J. Nührenberg,
Optimization of M=2 Stellarator; Dec. 1996

NIFS-471 A. Fujisawa, H. Iguchi, S. Lee and Y. Hamada,
Effects of Horizontal Injection Angle Displacements on Energy Measurements with Parallel Plate Energy Analyzer; Dec. 1996

NIFS-472 R. Kanno, N. Nakajima, H. Sugama, M. Okamoto and Y. Ogawa,
Effects of Finite-β and Radial Electric Fields on Neoclassical Transport in the Large Helical Device; Jan. 1997

NIFS-473 S. Murakami, N. Nakajima, U. Gasparino and M. Okamoto,
Simulation Study of Radial Electric Field in CHS and LHD; Jan. 1997

NIFS-474 K. Ohkubo, S. Kubo, H. Idei, M. Sato, T. Shimozuma and Y. Takita,
Coupling of Tilting Gaussian Beam with Hybrid Mode in the Corrugated Waveguide; Jan. 1997

NIFS-475 A. Fujisawa, H. Iguchi, S. Lee and Y. Hamada,
Consideration of Fluctuation in Secondary Beam Intensity of Heavy Ion Beam Prove Measurements; Jan. 1997

NIFS-476 Y. Takeiri, M. Osakabe, Y. Oka, K. Tsumori, O. Kaneko, T. Takanashi, E. Asano, T. Kawamoto, R. Akiyama and T. Kuroda,
Long-pulse Operation of a Cesium-Seeded High-Current Large Negative Ion Source; Jan. 1997

NIFS-477 H. Kuramoto, K. Toi, N. Haraki, K. Sato, J. Xu, A. Ejiri, K. Narihara, T. Seki, S. Ohdachi, K. Adati, R. Akiyama, Y. Hamada, S. Hirokura, K. Kawahata and M. Kojima,
Study of Toroidal Current Penetration during Current Ramp in JIPP T-IIU with Fast Response Zeeman Polarimeter; Jan., 1997

NIFS-478 H. Sugama and W. Horton,
Neoclassical Electron and Ion Transport in Toroidally Rotating Plasmas; Jan. 1997

NIFS-479 V.L. Vdovin and I.V. Kamenskij,
3D Electromagnetic Theory of ICRF Multi Port Multi Loop Antenna; Jan.

1997

NIFS-480 W.X. Wang, M. Okamoto, N. Nakajima, S Murakami and N. Ohyabu,
Cooling Effect of Secondary Electrons in the High Temperature Divertor Operation; Feb. 1997

NIFS-481 K. Itoh, S.-I. Itoh, H. Soltwisch and H.R. Koslowski,
Generation of Toroidal Current Sheet at Sawtooth Crash; Feb. 1997

NIFS-482 K. Ichiguchi,
Collisionality Dependence of Mercier Stability in LHD Equilibria with Bootstrap Currents; Feb. 1997

NIFS-483 S. Fujiwara and T. Sato,
Molecular Dynamics Simulations of Structural Formation of a Single Polymer Chain: Bond-orientational Order and Conformational Defects; Feb. 1997

NIFS-484 T. Ohkawa,
Reduction of Turbulence by Sheared Toroidal Flow on a Flux Surface; Feb. 1997

NIFS-485 K. Narihara, K. Toi, Y. Hamada, K. Yamauchi, K. Adachi, I. Yamada, K. N. Sato, K. Kawahata, A. Nishizawa, S. Ohdachi, K. Sato, T. Seki. T. Watari, J. Xu, A. Ejiri, S. Hirokura, K. Ida, Y. Kawasumi, M. Kojima, H. Sakakita, T. Ido, K. Kitachi, J. Koog and H. Kuramoto,
Observation of Dusts by Laser Scattering Method in theJIPPT-IIU Tokamak Mar. 1997

NIFS-486 S. Bazdenkov, T. Sato and The Complexity Simulation Group,
Topological Transformations in Isolated Straight Magnetic Flux Tube; Mar. 1997

NIFS-487 M. Okamoto,
Configuration Studies of LHD Plasmas; Mar. 1997

NIFS-488 A. Fujisawa, H. Iguchi, H. Sanuki, K. Itoh, S. Lee, Y. Hamada, S. Kubo, H. Idei, R. Akiyama, K. Tanaka, T. Minami, K. Ida, S. Nishimura, S. Morita, M. Kojima, S. Hidekuma, S.-I. Itoh, C. Takahashi, N. Inoue, H. Suzuki, S. Okamura and K. Matsuoka,
Dynamic Behavior of Potential in the Plasma Core of the CHS Heliotron/Torsatron; Apr. 1997